Complementary pair-density-wave and d-wave-checkerboard orderings in high-temperature superconductors

K. Seo H. D. Chen

J. P. Hu

Complementary pair-density-wave and *d*-wave-checkerboard orderings in high-temperature superconductors

Kangjun Seo,[1] Han-Dong Chen,[2] and Jiangping Hu[1]
[1]*Department of Physics, Purdue University, West Lafayette, Indiana 47907, USA*
[2]*Department of Physics, University of Illinois at Urbana-Champaign, Urbana, Illinois 61801, USA*
(Received 27 August 2007; revised manuscript received 29 June 2008; published 17 September 2008)

The competing orders in the particle-particle (P-P) channel and the particle-hole (P-H) channel have been proposed separately to explain the pseudogap physics in cuprates. By solving the Bogoliubov-de Gennes equation self-consistently, we show that there is a general complementary connection between the *d*-wave-checkerboard (DWCB) order in the P-H channel and the pair-density-wave (PDW) order in the P-P channel. A small pair density localization generates DWCB and PDW orders simultaneously. The result suggests that suppressing superconductivity locally or globally through phase fluctuation should induce both orders in underdoped cuprates. The presence of both DWCB and PDW orders with $4a \times 4a$ periodicity can explain the checkerboard modulation observed in Fourier transform scanning tunneling spectroscopies from scanning tunneling microscopy and the puzzling dichotomy between the nodal and antinodal regions as well as the characteristic features such as nondispersive Fermi arc in the pseudogap state.

DOI: 10.1103/PhysRevB.78.094510 PACS number(s): 74.25.Jb, 74.25.Dw, 74.72.−h

I. INTRODUCTION

An important characteristic of strongly correlated electron systems is the existence of different instabilities that lead to many competing orders. In high-temperature superconductors, besides the superconducting phase, many competing orders, such as spin-density wave (SDW),[1,2] *d*-density wave (DDW),[3,4] pair density wave (PDW),[5,6] stripe,[7] and so on, have been proposed to explain various experimental observations. Those competing orders can be generally classified into two categories: the orders in particle-particle (P-P) channel and the orders in the particle-hole (P-H) channel. So far, most of theoretical works in cuprates have focused on the effect of individual competing orders. However, the orders in two channels are not completely independent of each other. In some cases, they must be correlated. In this paper, we detailed study one of these examples, the extended *s*-wave PDW order in the P-P channel and the *d*-wave-checkerboard (DWCB) density order in the P-H channel.

The motivation of this study mainly comes from the recent experiments of scanning tunneling microscopy (STM) in cuprates. These experiments have revealed surprising yet important electronic structures in the high-temperature superconductors. The Fourier transform scanning tunneling spectroscopies (FT-STS) from STM have captured two different general features in both momentum and energy spaces.[8–16] One feature is dispersive peaks in FT-STS,[11,12] interpreted as interference patterns caused by elastic scattering of quasiparticles from impurities.[17] The other is nondispersive peaks, a checkerboard modulation observed in various different materials and circumstances. The checkerboard structure was first discovered locally in $Bi_2Sr_2CaCu_2O_{8+\delta}$ (BSCCO) near a vortex core.[8,18] Then, it was found to be a characteristic of the large gap regions where the STM spectrum resembles that in the pseudogap phase.[9,12,14] Later, in the pseudogap phase, a similar checkerboard pattern was also observed.[13] Finally, the STM studies of $Ca_{2-x}Na_xCuO_2Cl_2$ revealed the presence of a global long-range commensurate checkerboard order independent of doping.[10]

There have been various theoretical proposals to explain the nondispersive checkerboard modulations. Most of these proposals are related to the competing orders. In these theories, the origin of the nondispersive modulations are tied to the existence of particular order parameters. The theories include pair density modulation,[5,6,19–21] current-density modulation,[22,23] spin modulation,[2] stripe charge modulation,[7,24] impurity scattering,[25] and so on.

Among the proposed mechanisms, the pair density wave has been shown to capture important characteristics of the checkerboard density modulation. The mechanism of PDW derives from high pairing energy scale in cuprates. It suggests that, unlike the superconductivity of normal BCS type superconductors that can be destroyed by breaking Cooper pairs, the superconductivity in cuprates can be more easily weakened or destroyed by phase fluctuations than by pair breaking. Based on this argument, pair density localization[5] was first proposed to explain the local checkerboard modulation in the presence of impurity or vortex. Later, a global pair density wave was proposed to explain the checkerboard physics in the pseudogap state.[6,13] It has also been shown that the symmetry of the tunneling intensity can distinguish the pair density modulation from the conventional density modulation.[6] While the pair density modulation provides a good understanding of the experimental results, the theory does not cover two important characterizations of the tunneling experiments, namely, the dichotomy between nodal and antinodal regions and the Fermic arc.

Recently, we have proposed a *d*-wave-checkerboard density order in P-H channel.[26] The DWCB can be viewed as a natural extension of the *d*-density wave order proposed to explain pseudogap physics[3,4] and is only different from the latter in terms of order wave vectors. We have shown that the DWCB order must exist when the PDW order is present in the global *d*-wave superconducting state. Moreover, we have demonstrated that the DWCB captures many general features of the STM experimental results. It has been demonstrated that the DWCB order has little effect on the density

of state at low energy in the superconducting phase, but has a strong effect on the STM spectrum around the superconducting gap at high energy. This result naturally explains the puzzling dichotomy between the nodal and antinodal regions observed in STM (Ref. 14) and angle-resolved photoemission spectroscopy (APRES).[27] The DWCB order also preserves in FT-STS spectrum at the wave vectors $\mathbf{Q}=\{(\pi/2a,0),(0,\pi/2a)\}$ the same symmetry as that observed in the experiments. Moreover, the DWCB preserves the nodes in the single-particle spectrum and generates a Fermi arc with little dispersion around the nodal points at high temperature, which are consistent with the results from ARPES. The Fermi arc has been a signature of the pseudogap region and has been proposed to explain the checkerboard pattern observed in the pseudogap state.[28] Thus, the DWCB provides a physical origin of the Fermi arc.

In this paper, by solving the Bogoliubov-de Gennes equation self-consistently, we further demonstrate the results drawn in Ref. 26. We design a microscopic model with the space modulated density-density interaction. We show that from the self-consistent solutions of the Bogoliubov-de Gennes equations, a weak spatially modulated density-density interactions can generate the DWCB and the PDW orders simultaneously in general. The combination of these two orders captures many important features of the STM experimental results. We organized the rest of this paper as follows: In Sec. II we introduce the d-wave-checkerboard density order to study the electronic states in the disordered d-wave superconducting states and the pseudogap phase at a temperature above T_c. In Sec. III we show how the complementary connection between the density orderings in the particle-particle and the particle-hole channels are closely related in the order wave vector and the symmetries. In Sec. IV we study the orders in cuprates by calculating a full self-consistent Bogoliubov-de Gennes (BdG) equation including DWCB and PDW in the d-wave superconducting state. In Sec. V we calculate the local density of states and the spectral weights in the presence of both DWCB and PDW and compare the recent experimental data.

II. d-WAVE-CHECKERBOARD DENSITY ORDER IN CUPRATES

In this section, we shall introduce the DWCB order and discuss its roles in different regions of the phase diagram in high-temperature superconductors. In Ref. 26, we have proposed a DWCB to explain the experimental results observed in the STM measurements in a global d-wave superconducting state. It has been shown that the presence of DWCB and competition with d-wave superconducting (DSC) order can capture the physics in a disordered superconducting state and in the pseudogap phase at a temperature above T_c. Here we present a more detailed discussion and analysis. First, we will show the average density of states (DOS) and the Fourier component at the order wave vector $\mathbf{Q}=\{(\pi/2,0),(0,\pi/2)\}$ calculated in a mixed state of DSC and DWCB orders show good agreements with experiments such as the spatially modulated local density of state (LDOS) in the disordered superconductors. Second, we will show that the presence of the DWCB order with the d-wave superconducting order at a higher temperature above T_c plays an important role in understanding the physics of the pseudogap phase: an emergence of the energy-independent Fermi arcs above T_c and the linear dependence of its length on temperature.

The mean-field Hamiltonian for the system where the DWCB coexists with d-wave superconducting order is given by

$$\mathcal{H}_{\mathrm{MF}}=\mathcal{H}_0+\mathcal{H}_{\mathrm{DWCB}}, \tag{1}$$

where

$$\mathcal{H}_0=\sum_{\mathbf{k},\sigma}\xi_{\mathbf{k}}c^{\dagger}_{\mathbf{k}\sigma}c_{\mathbf{k}\sigma}+\sum_{\mathbf{k}}\Delta_{\mathbf{k}}c^{\dagger}_{\mathbf{k}\uparrow}c^{\dagger}_{-\mathbf{k}\downarrow}+\mathrm{H.c.}, \tag{2}$$

$$\mathcal{H}_{\mathrm{DWCB}}=\sum_{\mathbf{k},\mathbf{q},\sigma}W_{\mathbf{k},\mathbf{q}}c^{\dagger}_{\mathbf{k}+\mathbf{q}\sigma}c_{\mathbf{k}\sigma}+\mathrm{H.c.} \tag{3}$$

$\mathcal{H}_0$ is the mean-field Hamiltonian for the d-wave superconducting state and thus $\Delta_{\mathbf{k}}=\Delta_0/2(\cos k_y-\cos k_y)$. The DWCB has particular order wave vectors $\mathbf{Q}=\{(\pi/2,0),(0,\pi/2)\}$ and can be written as $W_{\mathbf{k},\mathbf{q}}=W_{\mathbf{k}}\delta_{\mathbf{q},\mathbf{Q}}$ with $W_{\mathbf{k}}=W_0/2(\cos k_x-\cos k_y)$.

To obtain a clear picture of the DWCB, we rewrite $\mathcal{H}_{\mathrm{DWCB}}$ in the real-space configuration

$$\begin{aligned}\mathcal{H}_{\mathrm{DWCB}}=&\sum_{\mathbf{r}}\mathrm{Im}(W_0)\left[\left(\cos\frac{\pi x}{2}+\sin\frac{\pi x}{2}\right)\hat{J}^{x}_{\mathbf{r}}-x\leftrightarrow y\right]\\&+\mathrm{Re}(W_0)\left[\left(\cos\frac{\pi x}{2}-\sin\frac{\pi x}{2}+2\cos\frac{\pi y}{2}\right)\right.\\&\left.\times\hat{B}^{x}_{\mathbf{r}}-x\leftrightarrow y\right],\end{aligned} \tag{4}$$

where $\mathbf{r}=(x,y)a$, $\hat{B}^{x(y)}_{\mathbf{r}}=\Sigma_{\sigma}(c^{\dagger}_{\mathbf{r},\sigma}c_{\mathbf{r}+a\hat{x}(\hat{y}),\sigma}+\mathrm{H.c.})$ is the density operator defined in the nearest-neighbor bond between $\mathbf{r}$ and $\mathbf{r}+a\hat{x}(\hat{y})$ with $\hat{x}(\hat{y})$ unit vectors along $x(y)$ directions, and $\hat{J}^{x(y)}_{\mathbf{r}}=i\Sigma_{\sigma}(c^{\dagger}_{\mathbf{r},\sigma}c_{\mathbf{r}+a\hat{x}(\hat{y}),\sigma}-\mathrm{H.c.})$ is the current-density operator defined in the same bond as $\hat{B}^{x(y)}_{\mathbf{r}}$. Figure 1 shows a static pattern of the bond strength of the DWCB order $\langle\hat{B}_{\mathbf{r}}\rangle$. It is clear that the DWCB order defined in Eq. (4) has $4a\times4a$ periodicity and $d_{x^2-y^2}$ symmetry. Similar order parameters have been mentioned in Ref. 25.

A. DWCB in the disordered superconducting state

Based on the mean-field Hamiltonian, Eq. (1), we have calculated the averaged local density of states $\rho(\omega)$ and the Fourier component of local density states at $\mathbf{Q}=\{(\pi/2,0),(0,\pi/2)\}$, $\rho_{\mathbf{Q}}(\omega)$, in two band dispersions. The calculation results turned out to be rather general and insensitive to the bare band structures. The effective mean-field Hamiltonian, Eq. (1), can be rewritten by using Nambu formalism

$$\mathcal{H}_{\mathrm{MF}}=\sum_{\mathbf{k}}\psi^{\dagger}_{\mathbf{k}}H(\mathbf{k})\psi_{\mathbf{k}}, \tag{5}$$

where $\psi_{\mathbf{k}}=(c_{\mathbf{k}\uparrow},c_{\mathbf{k}+\mathbf{Q}\uparrow},c^{\dagger}_{-\mathbf{k}\downarrow},c^{\dagger}_{-\mathbf{k}-\mathbf{Q}\downarrow})^{\dagger}$ and

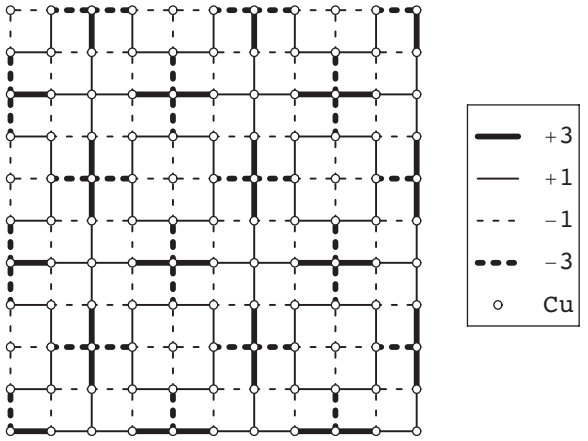

FIG. 1. The configuration of the bond density of the DWCB order in the real space. It is manifestly shown that the pattern has $4a \times 4a$ periodicity and $d_{x^2-y^2}$ symmetry.

$$H(\mathbf{k}) = \begin{pmatrix} \xi_{\mathbf{k}} & W_{\mathbf{k}} & \Delta_{\mathbf{k}} & 0 \\ W_{\mathbf{k}}^* & \xi_{\mathbf{k+Q}} & 0 & \Delta_{\mathbf{k+Q}} \\ \Delta_{\mathbf{k}}^* & 0 & -\xi_{-\mathbf{k}} & W_{\mathbf{k+Q}}^* \\ 0 & \Delta_{\mathbf{k+Q}}^* & W_{\mathbf{k+Q}} & -\xi_{-\mathbf{k+Q}} \end{pmatrix}. \tag{6}$$

Then the retarded Green function is given by

$$\mathbf{G}^{-1}(\mathbf{k},\omega) = (\omega + i\eta)\mathbf{I} - H(\mathbf{k}), \tag{7}$$

where $\mathbf{I}$ is the identity matrix with the same rank with $H(\mathbf{k})$. The averaged density of states and the Fourier component at $\mathbf{Q}$ can be calculated as the following, respectively:

$$\rho(\omega) = -\frac{1}{\pi}\sum_{\mathbf{k}} \mathrm{Im}\, \mathbf{G}_{11}(\mathbf{k},\omega), \tag{8}$$

$$\rho_{\mathbf{Q}}(\omega) = -\frac{1}{\pi}\sum_{\mathbf{k}} \mathrm{Im}\, \mathbf{G}_{12}(\mathbf{k},\omega). \tag{9}$$

First, we performed calculations in the particle-hole symmetric case, where the band dispersion is given by

$$\xi_{\mathbf{k}} = -t/2(\cos k_x + \cos k_y) - \mu. \tag{10}$$

We chose $t=125$ meV and $\mu=0$. $\Delta_0=40$ meV, which is relevant for underdoped BSCCO. The imaginary part of the self energy $\eta=5$ meV was used for the numerical calculation.

Figure 2(a) shows the averaged DOS normalized by one of the noninteracting Fermi liquids. In the absence of DWCB order, i.e., $W_0=0$, there are sharp coherence peaks at the energy of superconducting gap as expected. As DWCB order develops, the coherence peaks located at 40 meV are suppressed, while the spectrum at low energy remains unchanged. From $W_0=4$ meV the prominent peak begins to appear within the superconducting gap. Note that even small DWCB made a strong effect on the spectrum at high energy as W_0 increases.

Figure 2(b) shows the Fourier components of LDOS at the wave vectors $\mathbf{Q}=\{(\pi/2,0),(0,\pi/2)\}$. It is known[6] that

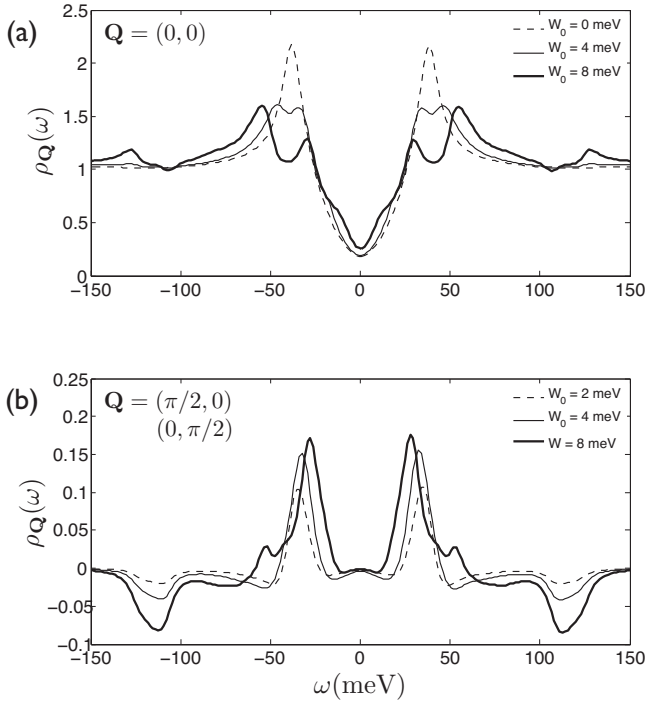

FIG. 2. (a) Averaged local density of states (LDOS) are plotted for various DWCB orders: $W_0=0,4$, and 8 meV with $t=-125$ meV, $t'=\mu=0$. (b) The Fourier components of LDOS at $\mathbf{Q}=\{(\pi/2,0),(0,\pi/2)\}$.

$\rho_{\mathbf{Q}}(\omega)=\rho_{\mathbf{Q}}(-\omega)$ for a bond-centered P-H pairing, while $\rho_{\mathbf{Q}}(\omega)=-\rho_{\mathbf{Q}}(-\omega)$ for a site-centered P-H pairing such as a conventional charge-density wave (CDW). As expected from the fact that the DWCB order is bond centered, $\rho_{\mathbf{Q}}(\omega)$ is even with respect to ω and it shows good agreement with experiment.[9]

We repeat our calculations with the more realistic band dispersion provided by Norman *et al.*[29] and the result is displayed at Fig. 3. The band energy dispersion is now modified as such

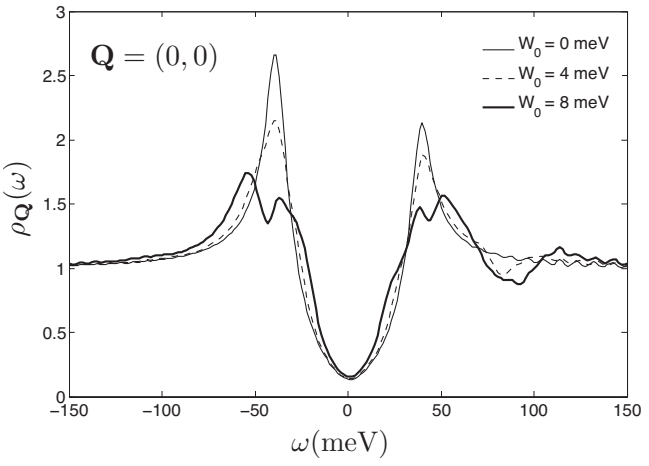

FIG. 3. Averaged local density of states with the finite chemical potential included in the band dispersion provided by Norman *et al.* (Ref. 29)

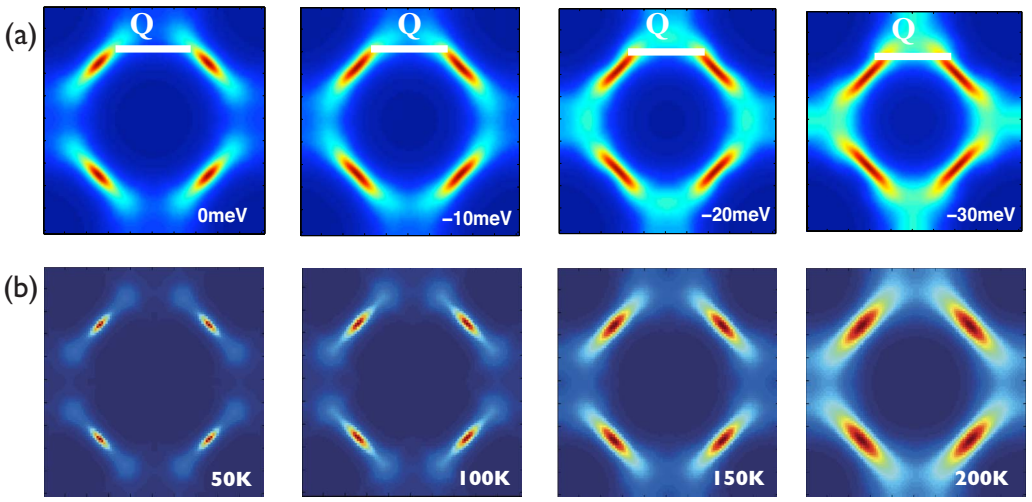

FIG. 4. (Color online) The spectral function given by Eq. (12) based on the energy dispersion Eq. (10). (a) The energy dependence of the Fermi arc along the Fermi surface. The white bars with the magnitude of $|\mathbf{Q}|=\pi/2$ are displayed to show the Fermi arc is nondispersive. The deviations for the energies ($\omega=0,-10,-20,-30$ meV) from $|\mathbf{Q}|$ are negligibly small by 8%, 2%, 0%, and 13% of $|\mathbf{Q}|$, respectively. (b) In the presence of DSC($\Delta_0=40$ meV) and DWCB($W_0=8$ meV), the spectral weights $A(\mathbf{k},\omega=0$ meV) are plotted with varying temperature ($T=50$, 100, 150, and 200).

$$\begin{aligned}\xi_{\mathbf{k}} &= t_1/2(\cos k_x + \cos k_y) + t_2 \cos k_x \cos k_y \\ &+ t_3/2(\cos 2k_x + \cos 2k_y) \\ &+ t_4/2(\cos 2k_x \cos k_y + \cos k_x \cos 2k_y) \\ &+ t_5 \cos 2k_x \cos 2k_y - \mu, \end{aligned} \tag{11}$$

where $t_1=-0.5951$ eV, $t_2=0.1636$ eV, $t_3=-0.0519$ eV, $t_4=-01117$ eV, and $t_5=0.0510$ eV.[29] The chemical potential μ is now set to -0.1660 eV. Compared with the P-H symmetric case, the effect of DWCB on the averaged DOS and the Fourier component of LDOS at $\mathbf{Q}$ is insensitive to the energy-band structure. Qualitatively the numerical results are strikingly consistent with experimental results,[16] and the large gap region can be interpreted in terms of the coexistence of weak (8–12 meV) DWCB and DSC orders.

B. DWCB in the pseudogap state

The results of LDOS have demonstrated the consistency between the coexistence of the DWCB and DSC orders and the STM experimental results in the disordered superconducting state. Now we will show that the presence of the DWCB order also captures important physics in the pseudogap phase at a temperature above T_c. While there still have been hot debates over the interpretation of the origin of the pseudogap phase, we will show how many experimental observations in this phase can be explained by interpreting the pseudogap phase as the mixed state of the DWCB and DSC orders. In this paper, we will focus on two features of the Fermi arcs developed from the nodal point along the Fermi surface: nondispersive energy independence and linear temperature dependence.

The autocorrelation of ARPES data from BSCCO show nondispersive peaks in momentum space arising from the tips of the Fermi arcs in the pseudogap phase, while the superconducting state shows dispersion with binding energy.[28] For the temperature dependence of the Fermi arcs in the pseudogap phase, it is known that its length increases linearly with temperature in the range between T_c and T^*, below which the material is believed to be in the pseudogap phase.[30] If the pseudogap phase is strongly connected to phase fluctuations of d-wave superconductivity, the single-particle spectrum should reflect the DWCB order. Therefore, a robust Fermi arc feature should exist in the mixed DWCB and DSC phases at high temperature. We will show that this is indeed the case.

In order to illustrate the emergence of the nondispersive Fermi arc in the pseudogap state with DWCB order coexistent with DSC, we have calculated the spectral function $A(\mathbf{k},\omega)$ as given by the imaginary part of the retarded Green function

$$A(\mathbf{k},\omega) = -\frac{1}{\pi}\mathrm{Im}\ \mathbf{G}_{11}(\mathbf{k},\omega). \tag{12}$$

First we have studied the energy dependence of the Fermi arcs in the pseudogap state. We have plotted the spectral function $A(\mathbf{k},\omega)$ in the first Brillouin zone in Fig. 4 based on the energy dispersion Eq. (10). In Fig. 4(a), the Fermi arcs are in red and one of the d-wave-checkerboard wave vectors $\mathbf{Q}=(\pi/2,0)$ is shown as a white bar. The scattering wave vectors connecting the tips of each arc are nearly equal to the order wave vectors of DWCB, $|\mathbf{Q}|=\pi/2$, which is consistent with the nondispersive Fermi arc in experimental observations. The small dispersion is negligible when compared with the elongation of the gapless part along the Fermi surface from the nodal point in the DSC state without DWCB order. It may depend on the bandwidth of the calculation. When including more hopping terms in the energy band, the dispersion shown in the simple band calculation will be reduced.

Now let us consider the temperature dependence of $A(\mathbf{k},\omega)$ at the Fermi level ($\omega=0$ meV). It can be calculated

in the pseudogap phase by taking the temperature dependence as an effect from the self-energy η. We have plotted the spectral function $A(\mathbf{k},\omega)$ as a function of the temperature in the first Brillouin zone in Fig. 4(b). At very low temperature the Fermi surface is gapped except at the nodal point $(\pi/2,\pi/2)$. As the temperature rises, the nodal points grow significantly along the Fermi surface with slight broadening in the direction perpendicular to the Fermi surface. We will show the detailed calculations and discuss more in Sec. V.

III. COMPLEMENTARY CONNECTION BETWEEN THE ORDERS IN THE P-P AND P-H CHANNELS

In this section, we will give a general argument regarding the complementary connection between the orders in the particle-particle and the particle-hole channels in the disordered *d*-wave superconducting state at zero temperature as well as in the pseudogap phase at high temperature above T_c. As shown above, a *d*-wave-checkerboard order in the P-H channel $\langle c^\dagger_{\mathbf{k}\sigma} c_{\mathbf{k+Q}\sigma}\rangle = \Phi f(\mathbf{k})$ with $\mathbf{Q}=\{(\pi/2,0),(0,\pi/2)\}$ and $f(\mathbf{k})=\cos k_x - \cos k_y$ can explain the experiments on cuprates in the disordered DSC state and in the pseudogap phase. Preserving the same symmetry in FT-STS spectrum as that observed in experiments, the DWCB generates Fermi arcs with little dispersion with the binding energy around nodal points at high temperature above T_c. Since the Fermi arc has been a signature of the pseudogap, the DWCB provides a direct link between the competing order and the pseudogap physics.

The DWCB, however, is not a completely independent mechanism. In fact, there are some intimate connections with other orders in the P-P channel. Due to the existence of a complementary connection between orders in both channels, the DWCB is directly connected to the PDW order. The angular symmetry of one orderings is determined by the combination of the angular symmetries of DSC and the complementary order. In this section, we will study how these density orderings in both channels are related in the modulation wave vector and the symmetry.

A. Connection between PDW and DDW

To show the connection, we will use the example of the *d*-density wave order. Since the density order in the P-H channel has been well studied, examining the complementary connected ordering in the P-P channel will be a preliminary step to generalize the complementary connection in the case of DWCB.

The mean-field Hamiltonian in the DSC state coexisting with DDW can be written as

$$\mathcal{H} = \sum_{\mathbf{k}\sigma} \xi_{\mathbf{k}} c^\dagger_{\mathbf{k}\sigma} c_{\mathbf{k}\sigma} + iW_{\mathbf{k}} c^\dagger_{\mathbf{k}\sigma} c_{\mathbf{k+Q}\sigma} + \sum_{\mathbf{k}} \Delta_{\mathbf{k}} c^\dagger_{\mathbf{k}\uparrow} c^\dagger_{-\mathbf{k}\downarrow} + \text{H.c.}$$
$$= \sum_{\mathbf{k}} \psi^\dagger(\mathbf{k}) A(\mathbf{k}) \psi(\mathbf{k}), \tag{13}$$

where $\psi^\dagger(\mathbf{k}) = (c_{\mathbf{k}\uparrow}\ c_{\mathbf{k+Q}\uparrow}\ c^\dagger_{-\mathbf{k}\downarrow}\ c^\dagger_{-\mathbf{k-Q}\downarrow})^\dagger$ and

$$A(\mathbf{k}) = \begin{pmatrix} \xi_{\mathbf{k}} & iW_{\mathbf{k}} & \Delta_{\mathbf{k}} & 0 \\ -iW_{\mathbf{k}} & -\xi_{\mathbf{k}} & 0 & -\Delta_{\mathbf{k}} \\ \Delta^*_{\mathbf{k}} & 0 & -\xi_{\mathbf{k}} & iW_{\mathbf{k}} \\ 0 & -\Delta^*_{\mathbf{k}} & -iW_{\mathbf{k}} & \xi_{\mathbf{k}} \end{pmatrix}, \tag{14}$$

where $c^\dagger_{\mathbf{k}\sigma}$ and $c_{\mathbf{k}\sigma}$ are the creation operator and destruction operator of the single particle with spin σ, respectively. $\xi_{\mathbf{k}}$ is the energy dispersion of the single particle. $\Delta_{\mathbf{k}} = \Delta_0/2(\cos k_x - \cos k_y)$ and $W_{\mathbf{k}} = W_0/2(\cos k_x - \cos k_y)$ are the *d*-wave superconducting order and the DDW, respectively. Then the Hamiltonian is diagonalized by the following transformation:

$$\begin{pmatrix} c_{\mathbf{k}\uparrow} \\ c_{\mathbf{k+Q}\uparrow} \\ c^\dagger_{-\mathbf{k}\downarrow} \\ c^\dagger_{-\mathbf{k-Q}\downarrow} \end{pmatrix} = \begin{pmatrix} \frac{-iW_{\mathbf{k}}}{\sqrt{2E_{\mathbf{k}}(E_{\mathbf{k}}-\xi_{\mathbf{k}})}} & \frac{\xi_{\mathbf{k}}+E_{\mathbf{k}}}{\sqrt{2E_{\mathbf{k}}(E_{\mathbf{k}}+\xi_{\mathbf{k}})}} & \frac{-iW_{\mathbf{k}}}{\sqrt{2E_{\mathbf{k}}(E_{\mathbf{k}}+\xi_{\mathbf{k}})}} & \frac{\xi_{\mathbf{k}}-E_{\mathbf{k}}}{\sqrt{2E_{\mathbf{k}}(E_{\mathbf{k}}-\xi_{\mathbf{k}})}} \\ \frac{\xi_{\mathbf{k}}-E_{\mathbf{k}}}{\sqrt{2E_{\mathbf{k}}(E_{\mathbf{k}}-\xi_{\mathbf{k}})}} & \frac{-iW_{\mathbf{k}}}{\sqrt{2E_{\mathbf{k}}(E_{\mathbf{k}}+\xi_{\mathbf{k}})}} & \frac{\xi_{\mathbf{k}}+E_{\mathbf{k}}}{\sqrt{2E_{\mathbf{k}}(E_{\mathbf{k}}+\xi_{\mathbf{k}})}} & \frac{-iW_{\mathbf{k}}}{\sqrt{2E_{\mathbf{k}}(E_{\mathbf{k}}-\xi_{\mathbf{k}})}} \\ 0 & \frac{\Delta_{\mathbf{k}}}{\sqrt{2E_{\mathbf{k}}(E_{\mathbf{k}}+\xi_{\mathbf{k}})}} & 0 & \frac{\Delta_{\mathbf{k}}}{\sqrt{2E_{\mathbf{k}}(E_{\mathbf{k}}-\xi_{\mathbf{k}})}} \\ \frac{\Delta_{\mathbf{k}}}{\sqrt{2E_{\mathbf{k}}(E_{\mathbf{k}}-\xi_{\mathbf{k}})}} & 0 & \frac{\Delta_{\mathbf{k}}}{\sqrt{2E_{\mathbf{k}}(E_{\mathbf{k}}+\xi_{\mathbf{k}})}} & 0 \end{pmatrix} \begin{pmatrix} \gamma_1(\mathbf{k}) \\ \gamma_2(\mathbf{k}) \\ \gamma_3(\mathbf{k}) \\ \gamma_4(\mathbf{k}) \end{pmatrix}, \tag{15}$$

where $E_{\mathbf{k}} = \sqrt{\xi^2_{\mathbf{k}} + |\Delta_{\mathbf{k}}|^2 + W^2_{\mathbf{k}}}$. The eigenvalues $E_\alpha(\mathbf{k})$ corresponding to the eigenvectors $\gamma_\alpha(\mathbf{k})$ are given by

$$E_1(\mathbf{k}) = E_2(\mathbf{k}) = +E_{\mathbf{k}}, \tag{16}$$

$$E_3(\mathbf{k}) = E_4(\mathbf{k}) = -E_{\mathbf{k}}. \tag{17}$$

The ground state $|\Omega\rangle$ is defined by the following conditions:

$$\gamma_1(\mathbf{k})|\Omega\rangle = \gamma_2(\mathbf{k})|\Omega\rangle = 0, \tag{18}$$

$$\gamma_3^\dagger(\mathbf{k})|\Omega\rangle = \gamma_4^\dagger(\mathbf{k})|\Omega\rangle = 0. \tag{19}$$

Then nonzero expectation values of the bilinear operators of cs are

$$\langle c_{\mathbf{k}\uparrow}^\dagger c_{\mathbf{k}\uparrow}\rangle = v_{\mathbf{k}}^2 \frac{|\Delta_{\mathbf{k}}|^2}{|\Delta_{\mathbf{k}}|^2 + W_{\mathbf{k}}^2}, \tag{20}$$

$$\langle c_{\mathbf{k}\uparrow}^\dagger c_{-\mathbf{k}\downarrow}^\dagger\rangle = \frac{\Delta_{\mathbf{k}}}{2E_{\mathbf{k}}}, \tag{21}$$

$$\langle c_{\mathbf{k}\uparrow}^\dagger c_{\mathbf{k}+\mathbf{Q}\uparrow}\rangle = \frac{iW_{\mathbf{k}}}{E_{\mathbf{k}}}, \tag{22}$$

$$\langle c_{\mathbf{k}\uparrow}^\dagger c_{-\mathbf{k}-\mathbf{Q}\downarrow}^\dagger\rangle = v_{\mathbf{k}}^2 \frac{iW_{\mathbf{k}}\Delta_{\mathbf{k}}}{|\Delta_{\mathbf{k}}|^2 + W_{\mathbf{k}}^2}, \tag{23}$$

where $v_{\mathbf{k}}^2 = \frac{1}{2}(1 - \frac{\xi_{\mathbf{k}}}{E_{\mathbf{k}}})$. Note that in a DSC state without DDW, or $W_{\mathbf{k}} = 0$,

$$\langle c_{\mathbf{k}\uparrow}^\dagger c_{\mathbf{k}\uparrow}\rangle = \frac{1}{2}\left(1 - \frac{\xi_{\mathbf{k}}}{\sqrt{\xi_{\mathbf{k}}^2 + |\Delta_{\mathbf{k}}|^2}}\right). \tag{24}$$

Therefore, in the mixed state of the DSC $\langle c_{\mathbf{k}\uparrow}^\dagger c_{-\mathbf{k}\downarrow}^\dagger\rangle \propto \Delta_{\mathbf{k}}$ and DDW $\langle c_{\mathbf{k}\sigma}^\dagger c_{\mathbf{k}+\mathbf{Q}\sigma}\rangle \propto iW_{\mathbf{k}}$, a PDW order with the same wave vector $\mathbf{Q}$ is expected to exist naturally, whose symmetry is an extended s wave manifestly given by

$$\langle c_{\mathbf{k}\uparrow}^\dagger c_{-\mathbf{k}-\mathbf{Q}\downarrow}^\dagger\rangle \propto iW_{\mathbf{k}}\Delta_{\mathbf{k}} = \frac{iW_0\Delta_0}{4}(\cos k_x - \cos k_y)^2. \tag{25}$$

This indicates that the mixed state of DDW and DSC leads to the existence of PDW. This argument can also be applied to the state of DSC coexisting with PDW leading to DDW. Therefore the mixed state of DSC and DDW is nothing but a complementarily connected description of the mixed state of DSC and PDW.

B. Connection between PDW and DWCB

Given the close resemblance between DDW and DWCB, it is natural to expect that similar results also hold for the DWCB order, since the difference between DDW and DWCB is the order wave vector $\mathbf{Q}$. Due to the high energy scale of superconducting gap in high temperature superconductors (HTS), superconducting order (SC) can be destroyed or suppressed by phase fluctuations. Carrying out a similar analysis as Gossamer superconductors,[31] we can show how the complementary connection between PDW and DWCB arises in the low energy effective Hamiltonian that describes a system with pair modulation induced by phase fluctuations.

We start from a BCS Hamiltonian on a two-dimensional (2D) square lattice

$$\mathcal{H}_{\mathrm{BCS}} = \sum_{\mathbf{k},\sigma} \xi_{\mathbf{k}} c_{\mathbf{k},\sigma}^\dagger c_{\mathbf{k},\sigma} + \sum_{\mathbf{k}} \Delta_{\mathbf{k}} c_{\mathbf{k},\uparrow}^\dagger c_{-\mathbf{k},\downarrow}^\dagger + \mathrm{H.c.} \tag{26}$$

The superconducting vacuum is constructed by the Cooper pairs with opposite momentum and spin

$$|\Psi_{\mathrm{BCS}}\rangle = \hat{U}_{\mathrm{BCS}}|0\rangle \propto e^{\sum_{\mathbf{k}} \alpha_{\mathbf{k}} c_{\mathbf{k},\uparrow}^\dagger c_{-\mathbf{k},\downarrow}^\dagger}|0\rangle, \tag{27}$$

where $|\alpha_{\mathbf{k}}|^2 = \frac{E_{\mathbf{k}} - \xi_{\mathbf{k}} + \mu}{E_{\mathbf{k}} + \xi_{\mathbf{k}} - \mu}$ and $E_{\mathbf{k}} = \sqrt{\xi_{\mathbf{k}}^2 + |\Delta_{\mathbf{k}}|^2}$. A local pair fluctuation induced by disorder such as a vortex, impurities, or other factors will lead to a new ground state with nonzero supercurrent due to the uncertainty principle. In other words, a new ground state $|\Psi\rangle$ can be obtained from the BCS ground state $|\Psi_{\mathrm{BCS}}\rangle$ by applying a boost of the total momentum $\mathbf{q}$ of the Cooper pairs

$$|\Psi\rangle = e^{\eta \sum_{\mathbf{k},\mathbf{q}} (\Phi_{\mathbf{q}} c_{\mathbf{k}\uparrow}^\dagger c_{-\mathbf{k}+\mathbf{q}\downarrow}^\dagger - \Phi_{\mathbf{q}}^* c_{-\mathbf{k}+\mathbf{q}\downarrow} c_{\mathbf{k}\uparrow})}|\Psi_{\mathrm{BCS}}\rangle, \tag{28}$$

where η is a small parameter and $\Phi_{\mathbf{q}}$ is the structural factor of pair fluctuations determined phenomenologically. For a commensurate checkerboard modulation, $\Phi_{\mathbf{q}}$ will be peaked at the related total momenta $\mathbf{q}$ of the pair, that is $\mathbf{q} = \mathbf{Q} = \{(\pi/2, 0), (0, \pi/2)\}$: $\Phi_{\mathbf{q}} \sim \delta_{\mathbf{q},\mathbf{Q}}$.

The effective Hamiltonian associated with $|\Psi\rangle$ as a ground state can be obtained as, up to a first order η,

$$\mathcal{H}_{\mathrm{eff}} = \mathcal{H}_{\mathrm{BCS}} + \mathcal{H}_{\mathrm{kin}} + \mathcal{H}_{\mathrm{int}} + O(\eta^2), \tag{29}$$

where $\mathcal{H}_{\mathrm{kin}}$ and $\mathcal{H}_{\mathrm{int}}$ are additional terms generated by boosted kinetic and pair interaction terms, respectively, in Eq. (26). For a commensurate checkerboard modulation,

$$\begin{aligned}\mathcal{H}_{\mathrm{kin}} &= -\eta \sum_{\mathbf{k},\mathbf{q}} \xi_{\mathbf{k}} \Phi_{\mathbf{q}} (c_{\mathbf{k},\uparrow}^\dagger c_{-\mathbf{k}+\mathbf{q},\downarrow}^\dagger + c_{-\mathbf{k}+\mathbf{q},\uparrow}^\dagger c_{\mathbf{k},\downarrow}^\dagger) + \mathrm{H.c.} \\ &= \sum_{\mathbf{k}} \Delta_{\mathbf{k},\mathbf{Q}} (c_{\mathbf{k},\uparrow}^\dagger c_{-\mathbf{k}+\mathbf{q},\downarrow}^\dagger + c_{-\mathbf{k}+\mathbf{q},\uparrow}^\dagger c_{\mathbf{k},\downarrow}^\dagger) + \mathrm{H.c.},\end{aligned} \tag{30}$$

where $\Delta_{\mathbf{k},\mathbf{Q}} = -\eta \Sigma_q \xi_{\mathbf{k}} \Phi_q \sim \xi_{\mathbf{k}} \delta_{\mathbf{q},\mathbf{Q}}$ and it represents an extended s-wave density order in the P-P channel or PDW. Moreover,

$$\mathcal{H}_{\mathrm{int}} = \eta \sum_{\mathbf{k},\mathbf{q},\sigma} \Phi_{\mathbf{q}} \Delta_{\mathbf{k}} c_{\mathbf{k},\sigma}^\dagger c_{\mathbf{k}+\mathbf{q},\sigma} + \mathrm{H.c.} = \sum_{\mathbf{k},\sigma} W_{\mathbf{k}} c_{\mathbf{k},\sigma}^\dagger c_{\mathbf{k}+\mathbf{q},\sigma} + \mathrm{H.c.}, \tag{31}$$

where $W_{\mathbf{k}} = \eta \Sigma_{\mathbf{q}} \Phi_{\mathbf{q}} \Delta_{\mathbf{k}} \sim \Delta_{\mathbf{k}} \delta_{\mathbf{q},\mathbf{Q}}$ and it represents a d-wave density order in the P-H channel DWCB. The above derivation tells us that a d-wave-like ordering in the P-H channel effectively leads to Cooper pairs with a finite center of mass momentum.

IV. SELF-CONSISTENT CALCULATION FOR PDW AND DWCB

Due to the complementary connection between PDW and DWCB, it is suggestive to calculate a fully self-consistent Bogoliubov-de Gennes equation including both orders simultaneously. It has been argued that long-range interaction between charge carriers is very important in cuprates. PDW can be induced by the long-range interaction between hole pairs. In this section, we will show that a solution of a self-consistent calculation with modulating pair potential and nearest-neighbor interaction can lead to orderings in both P-P and P-H channels.

We start from a full model Hamiltonian on a 2D lattice

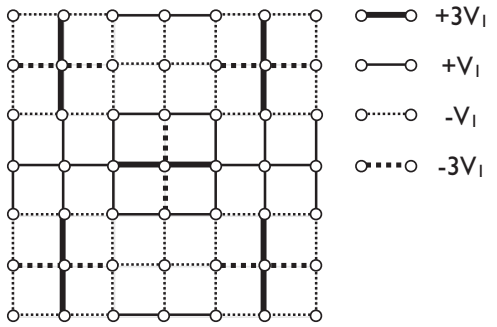

FIG. 5. A modulating nearest-neighbor interaction δV_{ij} is plotted in a 2D square lattice.

$$\mathcal{H} = -\frac{1}{2}\sum_{i,j,\sigma}[t_{ij}c_{i\sigma}^{\dagger}c_{j\sigma} + \text{H.c.}] + \sum_{i,j} V_{ij}n_i n_j - \mu\sum_i n_i, \tag{32}$$

where $n_i = n_{i\uparrow} + n_{i\downarrow}$.

In particular, we will consider nearest-neighbor hopping $t_{ij} = t$ and an attractive nearest-neighbor interaction V_{ij}. The chemical potential μ is chosen such that it is P-H symmetric case. The nearest-neighbor interactions between two opposite spins are considered to be attractive and modulating. They are given by a negative constant pair potential and a long-range interaction modulated by $\mathbf{Q} = \{(\pi/2, 0), (0, \pi/2)\}$,

$$V_{ij} = -V_0 + \delta V_{ij} = -V_0 + \sum_{\mathbf{Q}} \Delta V_{ij}(\cos \mathbf{Q}\cdot\mathbf{r}_i + \cos \mathbf{Q}\cdot\mathbf{r}_j), \tag{33}$$

where

$$\Delta V_{ij} = \begin{cases} +V_1, & j = i \pm \hat{x} \\ -V_1, & j = i \pm \hat{y}, \end{cases} \tag{34}$$

with V_0 and V_1 positive constants. While the local behavior of δV_{ij} seems to be anisotropic at the center and $(\pm 2a, \pm 2a)$ as seen in Fig. 5, the global behavior is isotropic in a sense that there is no preferential direction for attraction enhanced by negative modulation or weakened by positive modulation. The anisotropic modulation is rotationally invariant with the combination of translation by $4a$.

Starting with this Hamiltonian, let us derive the BdG equations by introducing mean-field decoupling of the nearest-neighbor interaction terms. The quartic term $n_{i\sigma}n_{j\sigma'}$ has three different types of mean-field decouplings

$$\begin{aligned} c_{i\sigma}^{\dagger}c_{i\sigma}c_{j\sigma'}^{\dagger}c_{j\sigma'} \Rightarrow\ & \langle c_{i\sigma}^{\dagger}c_{i\sigma}\rangle c_{j\sigma'}^{\dagger}c_{j\sigma'} + \langle c_{j\sigma'}^{\dagger}c_{j\sigma'}\rangle c_{i\sigma}^{\dagger}c_{i\sigma} \\ & + \langle c_{i\sigma}^{\dagger}c_{j\sigma'}^{\dagger}\rangle c_{j\sigma'}c_{i\sigma} + c_{i\sigma}^{\dagger}c_{j\sigma'}^{\dagger}\langle c_{j\sigma'}c_{i\sigma}\rangle \\ & - \langle c_{i\sigma}^{\dagger}c_{j\sigma'}\rangle c_{j\sigma'}^{\dagger}c_{i\sigma} - c_{i\sigma}^{\dagger}c_{j\sigma'}\langle c_{j\sigma'}^{\dagger}c_{i\sigma}\rangle. \end{aligned} \tag{35}$$

The first two terms are nothing but the chemical-potential terms. The decouplings in the second line are the usual BCS decouplings. The last two terms are decouplings in the P-H channel, which are just the exchange terms. For interactions between two particles with same spins, these exchange terms effectively modified hopping terms. For interactions between two particles with opposite spins, it corresponds to a bond-centered spin-density wave. From our full Hamiltonian, we can argue that the spin rotational symmetry is not broken. Thus the SDW decouplings can be safely ignored. Also, since we are interested in *d*-wave pairing, the BCS decouplings of triplet pairing will be dropped too. We then arrive at the following mean-field (MF) Hamiltonian:

$$\begin{aligned} \mathcal{H}_{\text{MF}} = & -\frac{1}{2}\sum_{\langle i,j\rangle\sigma}[(t + W_{ij})c_{i\sigma}^{\dagger}c_{j\sigma} + \text{H.c.}] + \sum_{\langle i,j\rangle}[\Delta_{ij}^{(1)}c_{i\uparrow}^{\dagger}c_{j\downarrow}^{\dagger} \\ & + \text{H.c.}] + \sum_{\langle i,j\rangle}[\Delta_{ij}^{(2)}c_{i\uparrow}^{\dagger}c_{j\downarrow}^{\dagger} + \text{H.c.}] - \sum_{\langle i,j\rangle\sigma}\mu_{ij\sigma}n_{i\sigma}, \end{aligned} \tag{36}$$

where

$$\Delta_{ij}^{(1)} = -V_0(\langle c_{j\downarrow}c_{i\uparrow}\rangle + \langle c_{i\downarrow}c_{j\uparrow}\rangle)/2, \tag{37}$$

$$W_{ij} = -\delta V_{ij}\langle c_{j\sigma}^{\dagger}c_{i\sigma}\rangle, \tag{38}$$

$$\Delta_{ij}^{(2)} = \delta V_{ij}(\langle c_{j\downarrow}c_{i\uparrow}\rangle + \langle c_{i\downarrow}c_{j\uparrow}\rangle)/2, \tag{39}$$

$$\mu_{ij\sigma} = \mu\delta_{ij} - V_{ij}\langle c_{j-\sigma}^{\dagger}c_{j-\sigma}\rangle, \tag{40}$$

The pairing amplitude on a bond (i,j), $\Delta_{ij}^{(1)}$, stems from a constant nearest-neighbor attraction $-V_0$ and the density wave pairings in the P-P and the P-H channels are caused by a long-range interaction δV_{ij}. Since our major interest is to study the orderings in both channels at the same time, the chemical potential $\mu_{ij\sigma}$ is taken to be a constant.

The Bogoliubov-de Gennes equation is given by

$$\begin{pmatrix} \mathcal{H}_0 & \Delta^* \\ \Delta & -\mathcal{H}_0^* \end{pmatrix}\begin{pmatrix} u_n(i) \\ v_n(i) \end{pmatrix} = E_n\begin{pmatrix} u_n(i) \\ v_n(i) \end{pmatrix}, \tag{41}$$

where $\mathcal{H}_0$ and Δ are transfer matrices such that

$$\mathcal{H}_0 x(i) = -\left[\sum_j (t + W_{ji}) + \mu_{ji}\right]x(j), \tag{42}$$

$$\Delta x(i) = \sum_j (\Delta_{ji}^{(1)} + \Delta_{ji}^{(2)})x(j), \tag{43}$$

where $x(i)$ can be either $u_n(i)$ or $v_n(i)$.

We numerically solve BdG eigenvalues E_n and eigenvectors $[u_n(i), v_n(i)]$ on a lattice of N sites with a periodic boundary condition. We then calculate the pairing amplitude and the density orderings in the P-P and the P-H channels which are, respectively, given by

$$\Delta_{ij}^{(1)} = -\frac{V_0}{2}\sum_n [u_n(j)v_n^*(i) + u_n(i)v_n^*(j)], \tag{44}$$

$$\Delta_{ij}^{(2)} = \frac{\delta V_{ij}}{2}\sum_n [u_n(j)v_n^*(i) + u_n(i)v_n^*(j)], \tag{45}$$

$$W_{ij} = -\delta V_{ij}\sum_n v_n(j)v_n^*(i). \tag{46}$$

Substituting these equations back into the BdG equation, Eq. (41), and repeating the same process until self-consistency is

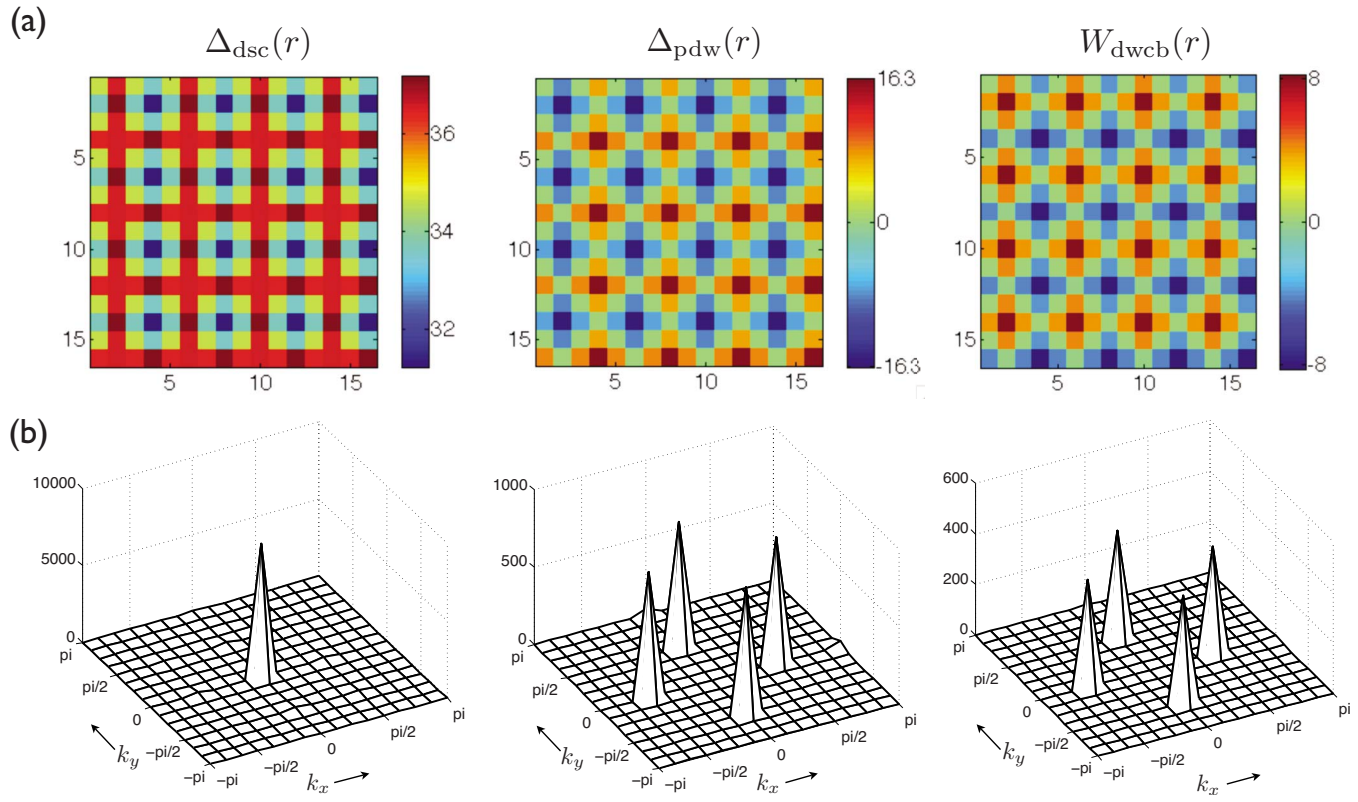

FIG. 6. (Color online) (a) The amplitude of the order parameters $\Delta_{\mathrm{DSC}}(r)$, $\Delta_{\mathrm{PDW}}(r)$, and $W_{\mathrm{DWCB}}(r)$ defined by Eqs. (47)–(49), respectively, plotted in 16×16 lattice sites. $\Delta_{\mathrm{DSC}}(r)\approx\Delta_0$, $\Delta_{\mathrm{PDW}}=\Delta_1\cos\mathbf{Q}\cdot r$, and $W_{\mathrm{DWCB}}(r)=W_0\cos\mathbf{Q}\cdot r$ with $\Delta_0=34.2$ meV, $\Delta_1=16.3$ meV, and $W_0=8.3$ meV, respectively. $t=125$ meV is chosen to have the amplitudes in units of meV. (b) The Fourier transforms of the order parameters are displayed in the first Brillouin zone. The prominent peaks are located at $\mathbf{Q}=\{(\pm\pi/2,0),(0,\pm\pi/2)\}$ in both PDW and DWCB.

achieved for each of the local variables, we can obtain solutions of the BdG equations. In the calculation, we have used Broyden's method for efficient iteration.

From the self-consistent solution, we can then compute the interesting order parameters. The d-wave pairing amplitude (DSC) at a lattice site $\mathbf{r}$ is determined by four nearest neighbors $\Delta_{ij}^{(1)}$:

$$\Delta_{\mathrm{DSC}}(\mathbf{r})=(\Delta_{\mathbf{r},\mathbf{r}+\hat{x}}^{(1)}+\Delta_{\mathbf{r},\mathbf{r}-\hat{x}}^{(1)}-x\leftrightarrow y)/4. \tag{47}$$

In the same way, an extended s-wave pairing density wave order in the P-P channels (PDW) can be obtained by $\Delta_{ij}^{(2)}$:

$$\Delta_{\mathrm{PDW}}(\mathbf{r})=(\Delta_{\mathbf{r},\mathbf{r}+\hat{x}}^{(2)}+\Delta_{\mathbf{r},\mathbf{r}-\hat{x}}^{(2)}+x\leftrightarrow y)/4, \tag{48}$$

and d-wave density ordering in the P-H channel (DWCB) is

$$W_{\mathrm{DWCB}}(\mathbf{r})=(W_{\mathbf{r},\mathbf{r}+\hat{x}}+W_{\mathbf{r},\mathbf{r}-\hat{x}}-x\leftrightarrow y)/4. \tag{49}$$

We shall now present our results of full calculation. The uniform part of the interaction is set to $V_0=-2.5t$ while the modulation part has amplitudes of V_1 with the range of $0.1t-1.0t$. The solutions we have obtained are independent of the initial guesses for the local variables. In Fig. 6(a), the order parameters $\Delta_{\mathrm{DSC}}(\mathbf{r})$, $\Delta_{\mathrm{PDW}}(\mathbf{r})$, and $W_{\mathrm{DWCB}}(\mathbf{r})$ in a 2D real space are plotted for $V_0=2.5t$ and $V_1=0.5t$ with $t=125$ meV. The P-H channel ordering $W_{\mathbf{r},\mathbf{r}'}$ shows d-wave symmetry such that

$$W_{\mathbf{r},\mathbf{r}'}=\begin{cases}W_0(\cos\mathbf{Q}\cdot\mathbf{r}+\cos\mathbf{Q}\cdot\mathbf{r}'), & \mathbf{r}'=\mathbf{r}\pm\hat{x}\\ -W_0(\cos\mathbf{Q}\cdot\mathbf{r}+\cos\mathbf{Q}\cdot\mathbf{r}'), & \mathbf{r}'=\mathbf{r}\pm\hat{y},\end{cases} \tag{50}$$

where $W_0=0.06t=8.3$ meV and the order wave vectors $\mathbf{Q}=\{(\pm\pi/2,0),(0,\pm\pi/2)\}$ as shown in Fig. 6(b).

The order in P-P channel has both d-wave $\Delta_{\mathbf{r},\mathbf{r}'}^{(1)}$ and extended s-wave $\Delta_{\mathbf{r},\mathbf{r}'}^{(2)}$ part. The extended s-wave part is a pure modulation described by

$$\Delta_{\mathbf{r},\mathbf{r}'}^{(2)}=\begin{cases}\Delta_1(\cos\mathbf{Q}\cdot\mathbf{r}+\cos\mathbf{Q}\cdot\mathbf{r}'), & \mathbf{r}'=\mathbf{r}\pm\hat{x}\\ \Delta_1(\cos\mathbf{Q}\cdot\mathbf{r}+\cos\mathbf{Q}\cdot\mathbf{r}'), & \mathbf{r}'=\mathbf{r}\pm\hat{y},\end{cases} \tag{51}$$

where $\Delta_1=0.13t=16.3$ meV and the same order wave vectors $\mathbf{Q}$. We have also obtained the results of d-wave pairing amplitude or $\Delta_{\mathbf{r},\mathbf{r}\pm\hat{x}}^{(1)}=\Delta_0$ and $\Delta_{\mathbf{r},\mathbf{r}\pm\hat{y}}^{(1)}=-\Delta_0$ with $\Delta_0=0.28t$. In Fig. 7 the modulation amplitudes of $\Delta_{\mathrm{DSC}}(\mathbf{r})$, $\Delta_{\mathrm{PDW}}(\mathbf{r})$, and $W_{\mathrm{DWCB}}(\mathbf{r})$ were plotted as a function of V_1.

The self-consistent BdG calculation shows that there is indeed a complementary connection between the density order in the P-P channel (PDW) and in the P-H channel (DWCB). Since PDW and DWCB are based on the same modulating interaction δV_{ij}, not only PDW and DWCB should be present simultaneously with d-wave superconductivity but also the symmetries and order wave vector $\mathbf{Q}$ of both orders should be closely related to each other. There-

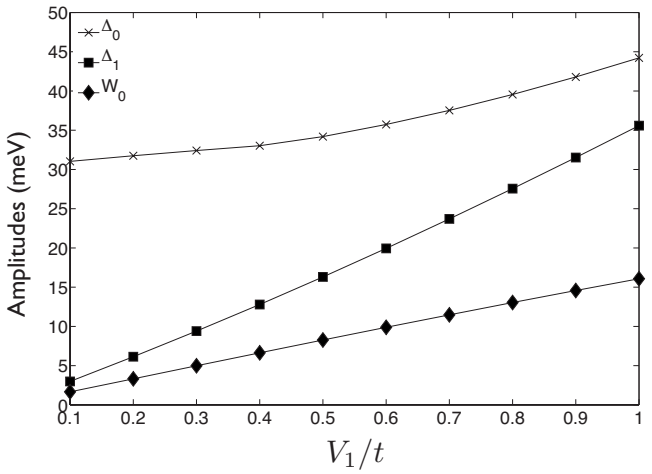

FIG. 7. The amplitudes, Δ_0, Δ_1, and W_0 of $\Delta_{\mathrm{DSC}}(r)$, $\Delta_{\mathrm{PDW}}(r)$, and $W_{\mathrm{DWCB}}(r)$, respectively, as a function of the modulation long-range interaction V_1. $t=125$ meV is chosen to have the amplitudes in units of meV. For a *d*-wave superconducting (DSC) order Δ_0 denoted by *x* along the curve for DSC, at each V_1 represents the mean value of $\Delta_{\mathrm{DSC}}(r)$ which is slightly modulated.

fore, the mean-field solutions in the disordered *d*-wave superconductivity should include a *d*-wave density wave with **Q** in the P-H pairing and an extended *s*-wave density wave with the same **Q** in the P-H pairing. Furthermore it is important to take both density orders into account on the same footing when we try to understand the electronic states of the disordered high T_c cuprates and the pseudogap state at high temperature.

V. THE MIXED DWCB AND PDW STATE

Analytically, the general features in STM measurements can be captured by the DWCB. Due to the anisotropy inherited from the *d*-wave factor of pairing, a weak DWCB order has a much stronger effect on the antinodal region than on the nodal region. Thus it naturally explains the puzzling dichotomy between the nodal and antinodal excitations in high-temperature superconductors. The local phase fluctuations of Cooper pairs lead to a local modulation of *d*-wave ordering in the P-H channel (DWCB), which strongly affects the antinodal single-particle excitations as well as an extended *s*-wave order in the P-P channel (PDW). Since both PDW and DWCB are bond centered, $\rho_{\mathbf{Q}}(\omega)$ will be an even function of ω.[6] This symmetry distinguishes the PDW and DWCB orders from the typical CDW in the P-H channel. The existing experimental results are consistent with the even case.

The purpose of this section is to determine the symmetries of density orders in P-P and P-H channels and then study the pseudogap physics under the presence of the orderings in P-P and P-H channels. Due to the complementary connection, if the PDW is an extended *s* wave, DWCB is a *d*-wave P-H pairing. If the PDW is a *d* wave, the P-H pairing density order must be extended *s* wave. It is worth noting that the symmetries of the orders are very important to explain the behavior of the conductance spectra at low energy. We will show that in DSC state the *d*-wave P-H pairing (DWCB) and the extended *s*-wave P-P pairing (PDW) can explain the low energy spectra while the solution with other symmetries cannot sufficiently match the experimental results.

In Sec. II, we have shown that, even without PDW, the presence of DWCB and DSC orders in a pseudogap state can capture the features of the Fermi arc. To understand the temperature dependence of the length of the Fermi arc above T_c we assumed the temperature dependence of the imaginary part of the energy η in the Green function implicitly. Using the results of the self-consistent calculations, this assumption of the temperature dependence of η is not necessary. The presence of the complementary connected *d*-wave orders in P-P and the extended *s*-wave order in P-H channels with DSC order naturally lead us to the temperature dependence of the length of the Fermi arc within the Franz and Millis model.[32]

A. Symmetries in P-P and P-H channels

In this subsection we study how the local density of states is associated with the symmetries of the complementary connected orders in P-P and P-H channels in a disordered *d*-wave superconducting state.

The local density of states in the DSC state in the presence of P-P and P-H channel orders is calculated by

$$\rho(\mathbf{r},\omega)=\sum_n [|u_n(\mathbf{r})|^2\delta(\omega-E_n)+|v_n(\mathbf{r})|^2\delta(\omega+E_n)]. \tag{52}$$

The averaged DOS is given by

$$\rho(\omega)=\sum_{\mathbf{r}}\rho(\mathbf{r},\omega) \tag{53}$$

and the Fourier components at the wave vectors $\mathbf{Q}=\{(\pi/2,0),(0,\pi/2)\}$ by

$$\rho_{\mathbf{Q}}(\omega)=\sum_{\mathbf{r}} e^{i\mathbf{Q}\cdot r}\rho(\mathbf{r},\omega). \tag{54}$$

We have calculated them in a simple band structure $t=-125$ meV and $\mu=0$.

For the *d*-wave P-H and extended *s*-wave P-P pairing, we have used $V_0=2.5t$ and various V_1 as in Eq. (55), where order parameters as solutions of the BdG calculation are given in meV, and δh is the height of $\rho(\omega)$ at $\omega=0$ off of the superconducting DOS displayed in a dashed line in Fig. 8.

V_1	Δ_{DSC}	Δ_{PDW}	W_{DWCB}	δh
$0.4t$	33.0	12.7	3.3	0.0599
$0.6t$	35.7	19.9	9.9	0.1125
$0.8t$	39.6	27.5	13.0	0.1445
$1.0t$	44.2	35.6	16.1	0.1546

(55)

For the extended *s*-wave P-H and *d*-wave P-P channel orders, we have used $V_0=2.5t$ and V_1 as in Eq. (56), where W_{SWCB} denotes the extended *s*-wave P-H pairing for convenience.

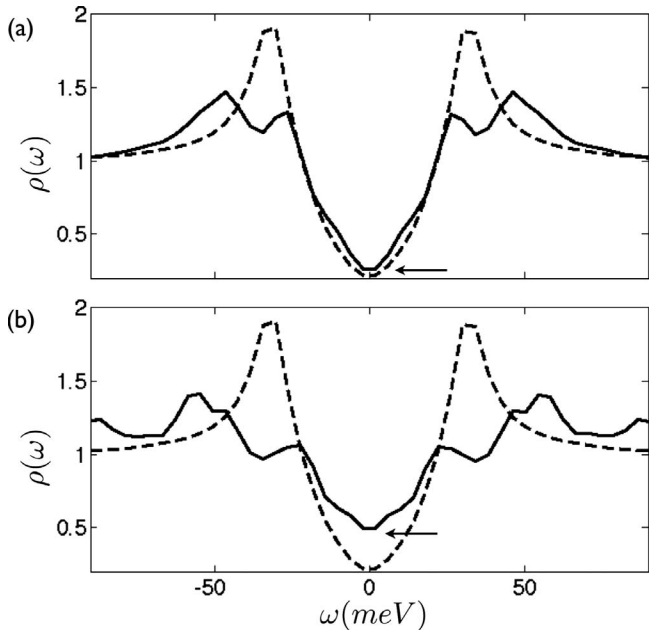

FIG. 8. (a) The averaged DOS are plotted for $\Delta_{DSC}=33$ meV in the case of d-wave P-H and extended s-wave P-P channel orders: $\Delta_{PDW}=12.7$ meV and $W_{DWCB}=3.3$ meV. The arrow indicates δh, that is, DOS at $\omega=0$ off of one for pure d-wave superconducting state. $\delta h=0.0599$. (b) The averaged DOS in the mixed state of DSC ($\Delta_{DSC}=33$ meV) with d-wave P-P and extended s-wave P-H channel orders. Here we plotted one with $\Delta_{PDW}=17.3$ meV and $W_{SWCB}=10$ meV. $\delta h=0.2933$.

V_1	Δ_{DSC}	Δ_{PDW}	W_{SWCB}	δh
$0.4t$	31.5	11.5	6.6	0.1144
$0.6t$	32.7	17.3	10.0	0.2933
$0.8t$	34.2	22.9	13.3	0.4200
$1.0t$	36.2	28.4	16.6	0.3589

(56)

The BdG calculation shows that DWCB, which is d-wave P-H pairing order, is crucial to the physics in the disordered superconductor. It captures the experimental observation of conductance spectrum at both low and high energies. As expected, the d-wave symmetry of the P-H pairing density order has little effect at low energy while it strongly affects the superconducting coherence peaks. Therefore we can conclude that the competing order in the P-H channel must have d-wave symmetry. Due to the complementary connection in the orders in P-H and P-P channels, it naturally leads to the existence of the pair density order that has extended s-wave symmetry.

In Fig. 8, to illustrate the above argument, we plotted the averaged DOS in two cases: (a) d-wave P-H and extended s-wave P-P channel orders and (b) s-wave P-H and extended d-wave P-P channel orders in the d-wave superconducting state ($\Delta_{DSC}=33$ meV).

B. The DWCB and PDW in the pseudogap state

Now let us consider the spectral function $A(\mathbf{k},\omega)$ in the pseudogap state to capture the features in the Fermi arc. First we rewrite the mean-field Hamiltonian for PDW and DWCB in momentum space. Taking the Fourier transform of Eq. (36), we obtain

$$\mathcal{H}_{PDW}=\sum_{\mathbf{r},\delta,\sigma}\Delta^{(2)}_{\mathbf{r},\mathbf{r}+\delta}c^{\dagger}_{\mathbf{r},\sigma}c^{\dagger}_{\mathbf{r}+\delta,-\sigma}+\text{H.c.}$$
$$=\sum_{\mathbf{p},\mathbf{q},\sigma}\left[\sum_{\mathbf{r},\delta}\Delta^{(2)}_{\mathbf{r},\mathbf{r}+\delta}e^{-i(\mathbf{p}+\mathbf{q})\cdot\mathbf{r}}e^{-i\mathbf{q}\cdot\delta}\right]c^{\dagger}_{\mathbf{p},\sigma}c^{\dagger}_{\mathbf{q},-\sigma}, \quad (57)$$

where δ denotes the unit vectors for the nearest neighbors of $\mathbf{r}$. Since $\Delta^{(2)}_{\mathbf{r},\mathbf{r}+\delta}=\Delta_1/2\Sigma_{\mathbf{Q}}[\cos\mathbf{Q}\cdot\mathbf{r}+\cos\mathbf{Q}\cdot(\mathbf{r}+\delta)]$, the term in the square bracket in Eq. (57) is rewritten as

$$\Delta_1\sum_{\mathbf{r},\mathbf{Q},\delta}[\cos\mathbf{Q}\cdot\mathbf{r}+\cos\mathbf{Q}\cdot(\mathbf{r}+\delta)]e^{-i(\mathbf{p}+\mathbf{q})\cdot\mathbf{r}}e^{-i\mathbf{q}\cdot\delta}$$
$$=\Delta_1\sum_{\mathbf{Q},\delta}(e^{-i\mathbf{q}\cdot\delta}+e^{i\mathbf{p}\cdot\delta})\delta_{\mathbf{p}+\mathbf{q},\mathbf{Q}}=\Delta_1\sum_{\mathbf{Q}}[\cos p_x+\cos(p_x+Q_x)$$
$$+x\leftrightarrow y]\delta_{\mathbf{p}+\mathbf{q},\mathbf{Q}}.$$

Thus $\mathcal{H}_{PDW}$ in momentum space can be given by

$$\mathcal{H}_{PDW}=\sum_{\mathbf{k},\mathbf{Q},\sigma}\Delta^{(2)}_{\mathbf{k}}c^{\dagger}_{\mathbf{k},\sigma}c^{\dagger}_{-\mathbf{k}-\mathbf{Q},-\sigma}+\text{H.c.}, \quad (58)$$

where $\Delta^{(2)}_{\mathbf{k}}=\Delta_1[\cos k_x+\cos(k_x+Q_x)+x\leftrightarrow y]$.

The momentum space expressions for DWCB in $\mathcal{H}_{MF}$, Eq. (36), can be obtained in the same way:

$$\mathcal{H}_{DWCB}=\sum_{\mathbf{k},\mathbf{Q},\sigma}W_{\mathbf{k}}c^{\dagger}_{\mathbf{k}+\mathbf{Q},\sigma}c_{\mathbf{k},\sigma}+\text{H.c.}, \quad (59)$$

where $W_{\mathbf{k}}=W_0[\cos k_x+\cos(k_x+Q_x)-x\leftrightarrow y]$. Therefore the mean-field Hamiltonian, Eq. (36), can be recast in momentum space as

$$\mathcal{H}_{MF}=\sum_{\mathbf{k},\sigma}(\xi_{\mathbf{k}}c\mathbf{k},\sigma^{\dagger}c_{\mathbf{k},\sigma}+\Delta^{(1)}_{\mathbf{k}}c^{\dagger}_{\mathbf{k},\sigma}c^{\dagger}_{-\mathbf{k},-\sigma})$$
$$+\sum_{\mathbf{k},\mathbf{Q},\sigma}(\Delta^{(2)}_{\mathbf{k}}c^{\dagger}_{\mathbf{k},\sigma}c^{\dagger}_{-\mathbf{k}-\mathbf{Q},-\sigma}+W_{\mathbf{k}}c^{\dagger}_{\mathbf{k}+\mathbf{Q},\sigma}c_{\mathbf{k},\sigma})+\text{H.c.}, \quad (60)$$

where $\xi_{\mathbf{k}}=-t/2(\cos k_x+\cos k_y)-\mu$ and $\Delta^{(1)}_{\mathbf{k}}=\Delta_0/2(\cos k_x-\cos k_y)$. In the same way as in Sec. II, it can be re-expressed in terms of the Nambu formalism as such

$$\mathcal{H}_{MF}=\sum_{\mathbf{k}}\psi^{\dagger}_{\mathbf{k}}H(\mathbf{k})\psi_{\mathbf{k}}, \quad (61)$$

where $\psi_{\mathbf{k}}=(c_{\mathbf{k}\uparrow},c_{\mathbf{k}+\mathbf{Q}\uparrow},c^{\dagger}_{-\mathbf{k}\downarrow},c^{\dagger}_{-\mathbf{k}-\mathbf{Q}\downarrow})^{\dagger}$ and

$$H(\mathbf{k})=\begin{pmatrix}\xi_{\mathbf{k}} & W_{\mathbf{k}} & \Delta^{(1)}_{\mathbf{k}} & \Delta^{(2)}_{\mathbf{k}}\\ W^{*}_{\mathbf{k}} & \xi_{\mathbf{k}+\mathbf{Q}} & \Delta^{(2)}_{\mathbf{k}+\mathbf{Q}} & \Delta^{(1)}_{\mathbf{k}+\mathbf{Q}}\\ \Delta^{(1)*}_{\mathbf{k}} & \Delta^{(2)*}_{\mathbf{k}+\mathbf{Q}} & \xi_{-\mathbf{k}} & W^{*}_{\mathbf{k}+\mathbf{Q}}\\ \Delta^{(2)*}_{\mathbf{k}} & \Delta^{(1)*}_{\mathbf{k}+\mathbf{Q}} & W_{\mathbf{k}+\mathbf{Q}} & \xi_{-\mathbf{k}+\mathbf{Q}}\end{pmatrix}. \quad (62)$$

The spectral function is given by the imaginary part of the Green function

$$G_{11}(\mathbf{k},\omega)=\langle\Omega|[\omega+i\eta-H(\mathbf{k})]^{-1}_{11}|\Omega\rangle. \quad (63)$$

The ground state $|\Omega\rangle$ is defined by the state without quasiparticles. In the pseudogap phase, it can be calculated within the model of Franz and Millis:[32]

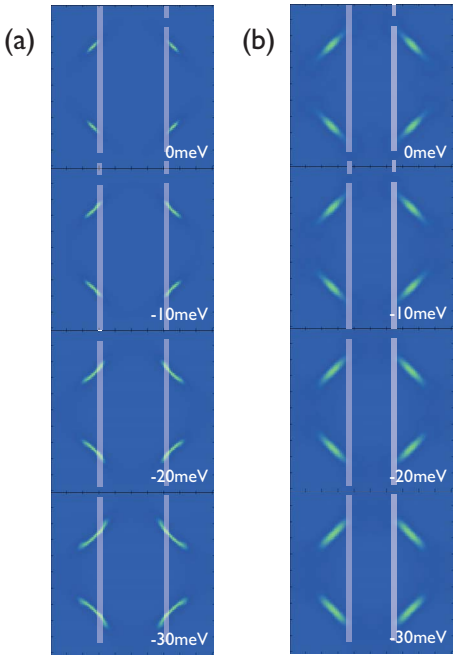

FIG. 9. (Color online) The energy dependence of the Fermi arc. (a) shows the development of the gapless region as a function of energy ω in the superconducting state without DWCB. As ω increases (from top to bottom), the scattering wave vectors connecting one tip of the green curve to another tip decrease. However, in (b) the gapless region remains unchanged as ω increases, that is, the Fermi arc is nondispersive.

$$A(\mathbf{k},\omega) = -\frac{1}{\pi}\int d\omega' P(\omega')\mathrm{Im}\, G_{11}(\mathbf{k},\omega-\omega'), \qquad (64)$$

where ω' is the energy shift due to the presence of a uniform supercurrent and $P(\omega')$ is the probability distribution of ω' calculated within a $2D$ XY model as such

$$P(\omega') = \sqrt{2\pi}W(T)e^{-\omega'^2/2W^2(T)}. \qquad (65)$$

where $W(T)$ is an order of pseudogap and an increasing function of temperature above T_c.

Now we will study the energy dependence of the Fermi arc in the pseudogap state. One of the salient features of the pseudogap phase is that the Fermi arc is nondispersive, whereas it is dispersive in the superconducting phase. The Fermi arc along the Fermi surface is identified by the peak of energy distribution curve (EDC) at $\omega=0$. Figure 9(b) demonstrates that the Fermi arc in green remains unchanged as ω is increased. In the superconducting state, however, the gapless region develops as the energy decreases below the Fermi level as seen in Fig. 9(a).

While the Fermi arc is nondispersive, it is found that the length of it is increasing linearly as a function of temperature.[30] Within the model of Franz and Millis, when $T>T_c$, $W(T)$ is an approximately linearly increasing function when the order parameters remain fixed. Adopting the values of $W(T)$ above T_c, we have calculated $A(\mathbf{k},\omega)$ as a function of temperature.

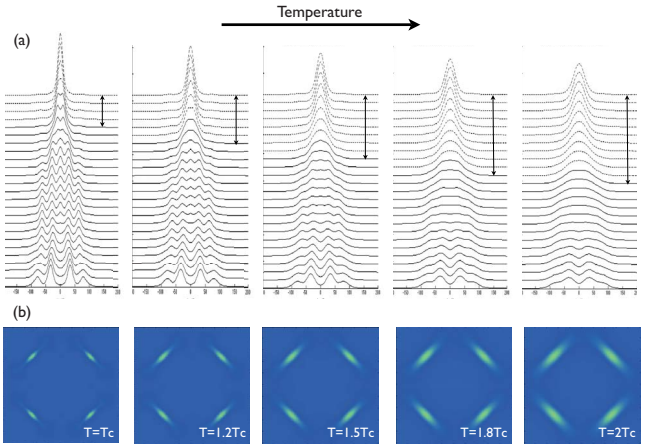

FIG. 10. (Color online) The temperature dependence of the Fermi arc above T_c. (a) EDCs along the Fermi surface from the nodal point (top) to antinodal point (bottom) are plotted. The arrows indicate the gapless part in the Fermi surface and show the length of the Fermi arc linearly depends on the temperature in the pseudogap state. (b) The Fermi arc as a function of the temperature T at above T_c.

In Fig. 10(a), EDC are plotted from the nodal to antinodal point along the Fermi surface. Clearly it shows a gapless nodal point and gapped antinodal point as indicated by darker curves. But, contrary to a superconducting state where the Fermi surface is gapped except at the nodal point, there is a region, the so-called Fermi arc, where peaks still survive at $\omega=0$ and thus the superconducting gap is closed. The curve on top is the EDC at the nodal point $(\pi/2,\pi/2)$ perpendicular to the Fermi surface. It is manifest that the size of the arrows is increasing as the temperature rises. Figure 10(b) shows the Fermi arc in the first Brillouin zone. As in the Fig. 9 the green color represents the gapless region of the Fermi surface, that is, the Fermi arc.

VI. CONCLUSION AND DISCUSSION

We have presented a detailed analysis of competing orders in cuprates which explains the checkerboard pattern observed in STM spectra. We have shown that in general there is a complementary connection between the orders in the P-P and the P-H channels in both the superconducting state and the pseudogap state. The symmetries of the orders in both channels are closely related to each other. In the d-wave superconducting state, the presence of the d-wave (extended s-wave) P-H density order implies the coexistence of the extended s-wave (d-wave) P-P pairing order. The self-consistent calculations in the disordered superconducting state result in solutions with uniform d-wave superconducting order, a P-H channel checkerboard density order with the order wave vector $\mathbf{Q}$, and a P-P channel pairing density wave with the same $\mathbf{Q}$. The symmetries of the channel orders are crucial to the effects on the density of states in STM experiments. We have found that d-wave-checkerboard density order in the P-P and the extended s-wave pair density wave are in good agreement with the experimental data in the superconducting phase.

The coexistence of orders in both P-P and P-H channels are important to understand the pseudogap phase which can be considered as a state which maintains pairing amplitude without phase coherence. The fluctuation of phase would naturally lead to the DWCB and PDW orders. We have shown that the presence of DWCB and PDW results in a nondispersive Fermi arc and our calculations show the linear dependence of the length of the Fermi arc at temperatures above T_c. Moreover, the effect of the presence of PDW and DWCB on single-particle spectra is much larger in the antinodal direction than in the nodal direction. These results also explain the dichotomy between the nodal and antinodal single-particle spectra in the cuprates.

The connections of the P-P and P-H channel orders are important in formulating the effective low energy theory in cuprates. From our results in this paper, the low energy effective theory should include both orders. So far, most theories have treated them independently. It is also clear that the presence of both orders can result in new physics in transport and thermal properties. A detailed study of these effects will be reported elsewhere.

ACKNOWLEDGMENTS

J.P.H. and K.S. are supported by National Scientific Foundation under Grant No. Phy-0603759. H.D.C. is supported by the U.S. Department of Energy, Division of Materials Sciences under Grant No. DEFG02-91ER45439, through the Frederick Seitz Materials Research Laboratory at the University of Illinois at Urbana-Champaign.

[1] S.-C. Zhang, Science **275**, 1089 (1997).
[2] S. Sachdev and E. Demler, Phys. Rev. B **69**, 144504 (2004).
[3] C. Nayak, Phys. Rev. B **62**, 4880 (2000).
[4] S. Chakravarty, R. B. Laughlin, D. K. Morr, and C. Nayak, Phys. Rev. B **63**, 094503 (2001).
[5] H. D. Chen, J. P. Hu, S. Capponi, E. Arrigoni, and S. C. Zhang, Phys. Rev. Lett. **89**, 137004 (2002).
[6] H. D. Chen, O. Vafek, A. Yazdani, and S. C. Zhang, Phys. Rev. Lett. **93**, 187002 (2004).
[7] S. A. Kivelson, I. P. Bindloss, E. Fradkin, V. Oganesyan, J. M. Tranquada, A. Kapitulnik, and C. Howald, Rev. Mod. Phys. **75**, 1201 (2003).
[8] J. E. Hoffman, E. W. Hudson, K. M. Lang, V. Madhavan, H. Eisaki, S. Uchida, and J. C. Davis, Science **295**, 466 (2002).
[9] C. Howald, H. Eisaki, N. Kaneko, M. Greven, and A. Kapitulnik, Phys. Rev. B **67**, 014533 (2003).
[10] T. Hanaguri, C. Lupien, Y. Kohsaka, D.-H. Lee, M. Azuma, M. Takano, H. Takagi, and J. C. Davis, Nature (London) **430**, 1001 (2004).
[11] K. McElroy, R. W. Simmonds, J. E. Hoffman, D.-H. Lee, J. Orenstein, H. Eisaki, S. Uchida, and J. C. Davis, Nature (London) **422**, 592 (2003).
[12] K. McElroy, J. E. Hoffman, D.-H. Lee, K. M. Lang, H. Eisaki, S. Uchida, and J. C. Davis, Physica C **388-389**, 225 (2003).
[13] M. Vershinin, S. Misra, S. Ono, Y. Abe, Y. Ando, and A. Yazdani, Science **303**, 1995 (2004).
[14] K. McElroy, D.-H. Lee, J. E. Hoffman, K. M. Lang, J. Lee, E. W. Hudson, H. Eisaki, S. Uchida, and J. C. Davis, Phys. Rev. Lett. **94**, 197005 (2005).
[15] K. McElroy, J. Lee, J. A. Slezak, D.-H. Lee, H. Eisaki, S. Uchida, and J. C. Davis, Science **309**, 1048 (2005).
[16] A. C. Fang, L. Capriotti, D. J. Scalapino, S. A. Kivelson, N. Kaneko, M. Greven, and A. Kapitulnik, Phys. Rev. Lett. **96**, 017007 (2006).
[17] Q.-H. Wang and D.-H. Lee, Phys. Rev. B **67**, 020511(R) (2003).
[18] S. H. Pan, E. W. Hudson, A. K. Gupta, K.-W. Ng, H. Eisaki, S. Uchida, and J. C. Davis, Phys. Rev. Lett. **85**, 1536 (2000).
[19] H.-D. Chen, S. Capponi, F. Alet, and S.-C. Zhang, Phys. Rev. B **70**, 024516 (2004).
[20] Z. Tesanovic, Phys. Rev. Lett. **93**, 217004 (2004).
[21] A. Melikyan and Z. Tesanovic, Phys. Rev. B **71**, 214511 (2005).
[22] C. Bena, S. Chakravarty, J. Hu, and C. Nayak, Phys. Rev. B **69**, 134517 (2004).
[23] A. Ghosal, A. Kopp, and S. Chakravarty, Phys. Rev. B **72**, 220502(R) (2005).
[24] J. A. Robertson, S. A. Kivelson, E. Fradkin, A. C. Fang, and A. Kapitulnik, Phys. Rev. B **74**, 134507 (2006).
[25] D. Podolsky, E. Demler, K. Damle, and B. I. Halperin, Phys. Rev. B **67**, 094514 (2003).
[26] K. Seo, H.-D. Chen, and J. Hu, Phys. Rev. B **76**, 020511(R) (2007).
[27] X. J. Zhou *et al.*, Phys. Rev. Lett. **92**, 187001 (2004).
[28] U. Chatterjee *et al.*, Phys. Rev. Lett. **96**, 107006 (2006).
[29] M. R. Norman, M. Randeria, H. Ding, and J. C. Campuzano, Phys. Rev. B **52**, 615 (1995).
[30] A. Kanigel *et al.*, Nat. Phys. **2**, 447 (2006).
[31] R. B. Laughlin, arXiv:cond-mat/0209269 (unpublished).
[32] M. Franz and A. J. Millis, Phys. Rev. B **58**, 14572 (1998).